

Chalkogenides of the transition elements. VI.¹ X-Ray, neutron, and magnetic investigation of the spinels Co_3O_4 , NiCo_2O_4 , Co_3S_4 , and NiCo_2S_4

OSVALD KNOP AND K. I. G. REID

Department of Chemistry, Dalhousie University, Halifax, Nova Scotia

AND

SUTARNO²

Department of Chemical Engineering, Nova Scotia Technical College, Halifax, Nova Scotia

AND

YASUAKI NAKAGAWA³

Department of Physics, Gakushuin University, Mejiro, Tokyo

Received February 13, 1968

The crystal structures of the spinels Co_3O_4 , NiCo_2O_4 , Co_3S_4 , and NiCo_2S_4 were refined from X-ray and neutron powder data. Their lattice parameters at room temperature and the positional parameters of the oxygen and sulfur atoms were: Co_3O_4 , $8.0835 \pm 6 \text{ \AA}$, 0.2640 ± 8 ; NiCo_2O_4 , $8.114 \pm 14 \text{ \AA}$, 0.2583 ± 34 ; Co_3S_4 , $9.4055 \pm 12 \text{ \AA}$, 0.2591 ± 5 ; NiCo_2S_4 , $9.3872 \pm 7 \text{ \AA}$, 0.2591 ± 3 . The thermal stabilities of the two oxides in air and in oxygen at 1 atm were investigated by thermogravimetric analysis and differential thermal analysis, and the magnetization of NiCo_2O_4 was measured down to 4.2°K in fields up to 11.70 kOe. From neutron diffraction NiCo_2O_4 was found to be inverse, while NiCo_2S_4 was shown to be normal. The results of the magnetization measurements and the neutron-diffraction patterns at 111 and 393°K were found to be equally consistent with the magnetic structure proposed for NiCo_2O_4 by Blasse, $\text{Co}^{2+}[\text{Ni}^{3+}\text{Co}^{3+}]\text{O}_4$ (Co^{2+} in a high-spin and Ni^{3+} and Co^{3+} in low-spin states), and with $\text{Co}^{3+}[\text{Ni}^{2+}\text{Co}^{3+}]\text{O}_4$ (Co^{3+} in $8(a)$ in a high-spin and Co^{3+} in $16(d)$ in a low-spin state). The sublattice magnetizations were not completely aligned even at 4.2°K ; the net magnetic moment derived from the magnetization measurements was only $1.25 \mu_B$, which is lower than the value of $2\mu_B$ expected from either model. At 111°K the moments of the ions in the tetrahedral and octahedral sites were estimated to be 1.9 ± 0.2 and -0.5 ± 0.1 bohr magnetons respectively.

Canadian Journal of Chemistry, 46, 3463 (1968)

Nickel in the cubic π phase Co_8NiS_8 shows no noticeable preference for octahedral coordination (1). It is of interest to know how common this lack of preference is in other sulfide structures based on a f.c.c. framework of sulfur atoms. The structure of the sulfospinel NiCo_2S_4 is of this type. It contains tetrahedrally and octahedrally coordinated metal atoms, but the distribution of Co and Ni in this compound has not been previously studied. An investigation of this sulfocobaltite was therefore undertaken. For comparison a similar investigation was carried out on the corresponding oxide, NiCo_2O_4 , which is magnetic at room temperature (2-4), and on the binary compounds Co_3S_4 and Co_3O_4 . All four

compounds have been described before, and some of them have been known for a long time (cf. Table I), but except for Co_3O_4 the positional parameters of the nonmetal atoms have never been determined.

Experimental

Preparation and Thermal Stability of the Oxides

Co_3O_4 was prepared by calcining reagent-grade cobalt carbonate at 700°C in air and allowing the product to cool slowly. The composition of cobalt carbonate is always uncertain, but thermogravimetric analysis (t.g.a.) showed that the carbonate was completely decomposed into Co_3O_4 between 550 and 600°C (Fig. 1). There was no further loss of weight until Co_3O_4 began to lose oxygen and decompose into CoO at about 950°C .

The diffraction pattern of the product, which was a very fine jet black powder, was well defined and contained no foreign lines. However, differential thermal analysis (d.t.a.) runs in stagnant air indicated onset of an endothermic process at about 660°C . The process was characterized by a composite peak terminating at about 1030°C (Fig. 1). Consequently the decomposition of Co_3O_4 into CoO cannot be simple, and Co_3O_4 may undergo some transformation below the calcining temperature, 700°C . At first glance the peak seems to consist of a small broad peak centering at about 900°C and a much narrower

¹For part V see ref. 21. A preliminary account of this work was read at the Chemical Institute of Canada Symposium on Structural Inorganic Chemistry in Halifax, N.S., September 1-3, 1965.

²Present address: Mineral Sciences Division, Mines Branch, Department of Energy, Mines and Resources, Ottawa, Canada.

³NRCC Postdoctorate Fellow in the Neutron Physics Branch, Atomic Energy of Canada Limited, Chalk River, Ont., 1962-63.

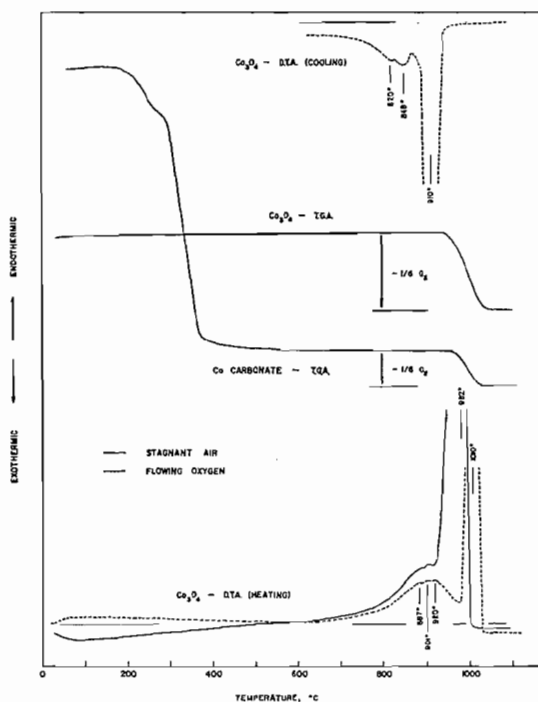


FIG. 1. T.g.a. and d.t.a. curves of cobalt carbonate and Co_3O_4 in stagnant air and in flowing oxygen. The t.g.a. curves are not on the same scale. D.t.a. peaks are cut off at half-widths. Weight changes in the t.g.a. curves refer to 1 CoO (final state on heating). Rate of heating, $6^\circ\text{C}/\text{min}$; rate of cooling, $6^\circ\text{C}/\text{min}$, then natural cooling.

main peak positioned at about 982°C . However, the profile of the composite peak is less symmetric than would correspond to an overlap of the two component peaks. In this the composite peak resembles somewhat the corresponding peak for NiCo_2O_4 (Fig. 2), the asymmetry of which is much more pronounced. A d.t.a. run in flowing oxygen gave a similar result, but the main peak was shifted to about 1010°C , while the broad peak remained essentially unchanged. The indications of fine structure of the broad peak are probably real, since they reappeared on cooling. The increased separation of the component peaks in oxygen showed that the main peak was symmetric.

There was no change in weight (within about ± 1 mg on a 0.5 g sample in stagnant air) that would correspond to the endothermic d.t.a. peak in the 660 – 920°C range, even when the usual uncertainties in correlating t.g.a. and d.t.a. curves are taken into account.

Even though the thermal hysteresis of the main d.t.a. peak in oxygen amounted to about 100°C , reoxidation of the CoO ultimately formed appeared to be fast and proceed through essentially the same stages as the decomposition of Co_3O_4 . This must also be the case on heating in air, as the final product obtained by the decomposition of the carbonate was single-phase Co_3O_4 . The calcining temperature employed in the preparation, 700°C , may perhaps have been too high, but the product reoxidized

completely during the slow cooling, and calcining at 700°C may have improved the crystallinity of the resulting oxide.

NiCo_2O_4 was prepared by dissolving the requisite amount of dried Co_3O_4 and NiO (reagent grade) in nitric acid, evaporating to dryness, and decomposing the residue on a hot plate till no more nitric fumes were given off. The resulting magnetic powder was ground and thoroughly mixed by repeated screening through a 325-mesh screen. To establish a maximum safe firing temperature the mixed oxide was investigated by t.g.a. in stagnant air and in flowing oxygen (Fig. 2). In air the loose powder (not dried) began to lose weight almost as soon as the heating started. A poorly defined plateau was reached at about 200°C ; at about 350°C a steady loss of weight set in. From there on there was a continuous and significant loss of oxygen till about 940°C . In oxygen the weight loss became appreciable at ca. 400°C , the shape of the t.g.a. curve being similar to that obtained in air but shifted by approximately 50°C towards higher temperatures. The composition of the final product above 950°C in air corresponded to NiCo_2O_3 , i.e. $(\text{Ni}_{1/3}\text{Co}_{2/3})\text{O}$.

When the t.g.a. residue was allowed to cool in the thermobalance from 1100°C in air, perceptible reoxidation began at ca. 830°C . The amount of oxygen absorbed in the reoxidation was less than $\frac{1}{2}\text{O}_2$ per formula unit of NiCo_2O_3 . Powder photographs of the cooled product contained strong but diffuse lines of a B1 pattern and reasonably sharp lines corresponding to the Co_3O_4 pattern. This would point to reoxidation of a homoge-

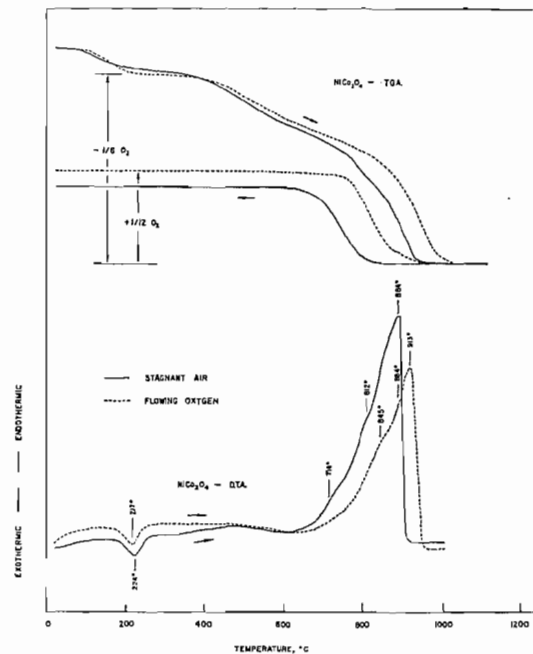


FIG. 2. T.g.a. and d.t.a. curves of NiCo_2O_4 (not dried) in stagnant air and in flowing oxygen. Weight changes in the t.g.a. curves refer to 1 $(\text{Ni}_{1/3}\text{Co}_{2/3})\text{O}$ (final state on heating). Rate of heating, $6^\circ\text{C}/\text{min}$; rate of cooling, $6^\circ\text{C}/\text{min}$ to about 500°C , then natural cooling.

neous solid-solution NiCo_2O_3 phase of the rock-salt type to a mixture of NiO , CoO , and Co_3O_4 , the lower oxides forming at least a limited solid solution.

From these results it was concluded that 300 °C in oxygen at atmospheric pressure would be a reasonable preparation temperature. Pressed disks of the nitrate calcine were fired for 7 days at 300 °C in flowing oxygen followed by slow cooling in the furnace. They crumbled readily to a very fine jet-black, strongly magnetic powder which gave a diffuse spinel pattern that could not be measured with satisfactory accuracy. The firing was repeated but the resulting patterns were still of poor quality. Both Co_3O_4 and NiCo_2O_4 were so fine that there was no need of grinding the powders to pass 400 mesh.

These results were in general agreement with the findings of Holgersson and Karlsson (2) who obtained, by firing the mixed nitrate at 850 °C in air, a homogeneous solid solution of CoO and NiO , while gentle heating over a Bunsen flame produced a spinel phase. However, Lotgering (4), who fired the nitrates at 300 °C in oxygen, remarks that though NiCo_2O_4 is unstable above about 400 °C, he was able to determine a reversible $1/\chi$ vs. temperature curve up to about 800 °C. Gocan (20) reported that he obtained magnetic spinel phases by calcining the mixed nitrates at 400, 500, 600, and 700 °C for 4 h, while at 800 °C a mixture of NiO , CoO (two separate phases), and Co_3O_4 resulted⁴.

To see if reversible reoxidation does take place on *slow* cooling, a specimen of NiCo_2O_4 was heated as loose powder at 700 °C for 2 days in flowing oxygen and then cooled to room temperature over 10 days without stopping the oxygen flow. The powder pattern of the product showed strong lines of a *B1* phase as well as a weaker line pattern that appeared to correspond to that of Co_3O_4 . Considering that at 700 °C the main loss of oxygen in our t.g.a. experiments had not yet taken place, our results are at variance with the findings of both Gocan and Lotgering.

Differential thermal analysis curves, in stagnant air and in flowing oxygen, of a NiCo_2O_4 specimen used for neutron diffraction showed similarities with the curves for Co_3O_4 , but the composite endothermic peaks were much more asymmetric, and even in oxygen there was no separation of the component peaks (Fig. 2). A puzzling feature, not present in the d.t.a. curves of Co_3O_4 , was a weak exothermic peak in the vicinity of 220 °C which appeared in air, oxygen, and purified argon, but only when virgin material was used. It was not observed on recycling. With the aid of infrared spectra of the oxide dispersed in KBr pellets it was eventually traced to small amounts of residual nitrate which was present even after the prolonged calcination. It seems that the initial loss of weight in the t.g.a. experiments (below say 300 or 350 °C) had its origin in the undecomposed nitrate and moisture.

Preparation of the Sulfides

Co_3S_4 and NiCo_2S_4 were prepared from Co_9S_8 or

⁴The lattice parameters of these spinels are given as 8.292, 8.316, 8.258, and 8.280 Å for the four temperatures employed, and that of Co_3O_4 is quoted as 8.180 Å. All these values are higher than any reported by other authors. They will be even higher when the wavelength used by Gocan, $\lambda(\text{CuK}\alpha) = 1.537$ Å, is converted to $\lambda(\text{CuK}\alpha) = 1.542$ Å.

Co_9NiS_8 , which were available in sufficient quantities from previous neutron-diffraction work (1), by adjusting the compositions with requisite amounts of sulfur and nickel and reacting the mixtures in evacuated silica ampuls. The reacted sulfides were ground to pass 100 mesh, mixed thoroughly by repeated screening, and resealed for homogenization (cf. ref. 1). This procedure was repeated when necessary. The resulting moderately sintered compacts were crushed to pass 100 mesh, except for the small amounts that were used for X-ray diffraction. These were ground carefully to pass 325 mesh.

X-Ray and Neutron Diffraction

X-Ray powder photography and measurement of integrated X-ray diffractometer intensities were carried out in a manner described elsewhere (18). Smear mounts were prepared by mixing the powders with silicone grease to a thick paste, pressing the paste into a shallow counterbore (0.4–0.6 mm deep) in a lucite slug, facing the paste with dry powder, and smoothing the resulting surface by gentle pressing against a microscope slide. Comparison with a pressed disk of NiCo_2O_4 showed that there was no gain in intensity on pressing, and smear mounts were used throughout. There was no evidence of preferred orientation. The wavelengths used were $\text{FeK}\alpha_1$, 1.93597 Å; $\text{FeK}\alpha$, 1.93728 Å; $\text{CoK}\alpha_1$, 1.78892 Å; and $\text{CoK}\alpha$, 1.79021 Å.

The neutron-diffraction experiments were performed at the NRX reactor of Atomic Energy of Canada Limited at Chalk River, Ont. As the investigation extended over 4 years, the diffraction patterns were obtained under a variety of conditions, not always strictly comparable. The neutron beam was monochromatized by Bragg reflection through 40° from the (111) plane of either an Al ($\lambda = 1.60$ Å) or a Ge crystal ($\lambda = 2.234$ Å). A single-crystal quartz filter 6 in. thick reduced the second-order (Al) and third-order (Ge) contents of the incident beam to less than 2%. A double-wall aluminium cryostat permitted measurements to be made at liquid-nitrogen and higher temperatures. Absorption corrections were determined from transmission measurements. In the more recent runs (Fig. 4) higher angular collimation was used. Other details are given in refs. 18 and 19.

The raw neutron-diffraction patterns were reduced to pF^2 patterns (19, 28). Overlapping peaks were resolved and Gaussian profiles fitted to all the peaks by a least-squares program written for the IBM 1620 (40K).

Least-Squares Refinement

The origin of the unit cell of the spinel structure (space group $Fd3m$) was taken at the center of symmetry. For a normal AB_2X_4 spinel there are 8 A atoms in 8(a): $\pm(1/8, 1/8, 1/8)$ etc.; 16 B in 16(d); and 32 X in 32(e): $\pm(xxx)$ etc., with x in the vicinity of $\frac{1}{2}$.

An ad hoc full-matrix program written for IBM 360/50 and weighting scheme W3 of ref. 21 were used in the refinements. A three-function interpolation scheme (22) was employed to compute the X-ray scattering factors from the equidistant values listed in refs. 23 (self-consistent field) and 24 (O^{2-}) after they had been corrected for dispersion (both parts) (25)⁵. Ionic scattering factors

⁵The dispersion correction for oxygen was taken from ref. 23 (CrK α).

TABLE I
Lattice parameters of the spinel cobaltites

Compound	a_0 , Å	Preparation	Reference
Co ₃ O ₄	8.05*		5
	8.07*	From nitrate; 700 °C	6
	8.124*	From nitrate by gentle heating; one diffuse doublet not indexed	2
	8.126*		7
	8.09		8
	8.070		3
	8.092	From nitrate; 750 °C/5 h in oxygen	4
	8.084		
	(24 °C)	From fluoride; 850 °C/24 h, $\lambda(\text{CoK}\alpha_1) = 1.7889$ Å	9
	8.083†		10
	8.0855 ± 5	From nitrate; calcined at 500 °C, ignited at 900 °C/240 h	11
	8.065	From CoO at 860 °C in oxygen; $\lambda(\text{CoK}\alpha) = 1.790$ Å	12
	8.0835 ± 6		This work
Co ₃ S ₄	9.38*		13
	9.401*		14
	9.416	From Co+S; 600 °C/24 h, 500 °C/60 h	4
	9.399 ± 2	From Co+S; 600 °C/24 h, 700 °C/70 h	15
NiCo ₂ O ₄	9.4055 ± 12	550 °C/4 days, 620 °C/3 days, slow cooling in furnace	This work
	8.128*	From nitrates (see footnote in text)	2
	8.098		3
	8.121	From nitrates; 300 °C/5 h in oxygen. Pattern not sharp, traces of a second phase (NiO ?)	4
	8.114 ± 14		This work
NiCo ₂ S ₄	9.392	From Ni+Co+S; 500 °C/10 h, 1000 °C/4 h, 1000 °C/4 h, (+S) 500 °C/48 h	4
	9.384 ± 2	From Ni+Co+S; 500 °C/24 h, 1000 °C/4 h, 500 °C/48 h	15
	9.3872 ± 7	500 °C/7 days, cooled to room temperature over 5 days (final heat treatment)	This work

* Adjusted to wavelengths used in this work. In refs. 2 and 7 it is not clear whether the units were Å or kX.
† Co oxalate dihydrate calcined in air at 500–750 °C/5 h. The product gave reproducible results, although gravimetric analysis and determination of the oxidizing power indicated a slight oxygen deficiency of the order of 1% (16).

were normally applied to the oxides and neutral to the sulfides. The neutron scattering amplitudes were taken from ref. 26 (for $b(\text{Co})$, however, see under Co₃O₄).

The same abbreviations are used in this paper as in ref. 21. The X-ray powder intensities of all four compounds have been submitted to the ASTM X-ray powder data file.

Magnetic Measurements

Intensities of magnetization of NiCo₂O₄ were measured, in the temperature range 4.2–533 °K, by the Faraday method using a magnetic balance. The balance was similar to that described by Hirone *et al.* (27) except that the deflection was detected by a mirror-photocell instead of a parallel-plate condenser system. At liquid-helium temperature the maximum magnetic field was limited to 8.60 kOe because of the larger pole gap required to accommodate the cryostat. At higher temperatures fields up to 11.70 kOe were used. The temperature of the powder specimen, which weighed about 10 mg, was measured with a calibrated AuCo–Cu thermocouple, ensuring good contact of the thermocouple with the powder. The balance was calibrated by measuring the magnetization of pure nickel powder.

Results and Discussion

Co₃O₄

The lattice parameter of our preparation agreed

well with most of the recent determinations (Table I). The possibility that a_0 depends somewhat on the method of preparation cannot be excluded (cf. ref. 3), so that the slight differences, within the range 8.08–8.09 Å, may be real.

A refinement from X-ray data based on the normal distribution, $\text{Co}^{2+}[\text{Co}_2^{3+}]\text{O}_4^{2-}$, and using individual isotropic temperature factors gave a physically reasonable result, though the temperature factors of both Co atoms were higher than one might expect (Table II). However, the same results were obtained when the refinement was started from widely different sets of initial parameter values or when a linear combination of $B(\text{O})$ and $x(\text{O})$ was introduced as an independent parameter to counteract the $B(\text{O})$ – $x(\text{O})$ correlation, which had the largest correlation coefficient, -0.65 .

No significant difference resulted when the structure was refined for an overall temperature factor (Table II) or when the inverse structure, $\text{Co}^{3+}[\text{Co}^{2+}\text{Co}^{3+}]\text{O}_4^{2-}$, was assumed. The $x(\text{O})$ value, 0.2637 ± 13 , compared favorably with

TABLE II
Results of the least-squares refinements from X-ray data (FeK α)*

After cycle	$B(\text{overall}), \text{\AA}^2$	$B(\text{A}), \text{\AA}^2$	$B(\text{B}), \text{\AA}^2$	$B(\text{X}), \text{\AA}^2$	$x(\text{X})$	K	$R, \%$	e.s.d. (w)
Co ²⁺ [Co ₂ ³⁺]O ₄ ²⁻ ($n = 15$)								
0		0.20	0.20	0.60	0.2600	1.000	10.47	7.42
10		1.02 ± 13	0.84 ± 10	1.16 ± 29	0.2637 ± 13	1.004 ± 13	2.01	1.17
0	1.00				0.2600	1.000	3.89	1.92
10	1.02 ± 6				0.2642 ± 10	0.995 ± 6	2.37	1.16
Co ³⁺ [Ni ²⁺ Co ³⁺]O ₄ ²⁻ ($n = 11$)								
0		0.20	0.20	0.60	0.2600	1.000	12.69	10.87
10		1.62 ± 63	1.00 ± 61	1.99 ± 127	0.2570 ± 45	0.987 ± 38	5.37	4.40
0	1.20				0.2600	1.000	6.20	4.22
3	1.16 ± 23				0.2593 ± 38	1.002 ± 25	6.25	4.19
Co[Co ₂]S ₄ ($n = 15$)								
0		0.45	0.20	0.45	0.2600	1.000	3.19	3.32
10		0.11 ± 18	0.27 ± 27	0.39 ± 27	0.2587 ± 6	0.987 ± 12	1.89	1.76
0	0.45				0.2600	1.000	3.94	3.91
8	0.25 ± 9				0.2594 ± 6	0.991 ± 9	2.31	1.83
Ni[Co ₂]S ₄ ($n = 16$)								
0		0.20	0.20	0.60	0.2600	1.000	2.83	2.64
10		0.50 ± 14	0.14 ± 17	0.57 ± 17	0.2589 ± 3	0.990 ± 7	1.55	1.20
0	0.30				0.2600	1.000	2.82	2.26
10	0.33 ± 7				0.2592 ± 3	0.993 ± 7	1.65	1.28

*Only results for the best models are listed here. For other models tried see text. First line, initial parameter values; second line, final parameter values.

that obtained by Roth (12) from CoK α intensities, 0.263⁶.

Only 9 single $|F_o|$ could be extracted from the neutron-diffraction pattern of Co₃O₄ (Fig. 3) by Gaussian analysis. Correction for second-order contamination was obtained from 400/2, which is a wholly second-order peak. It amounted to about 0.8% of the first-order reduced intensity. Refinement from these limited data was rendered even less favorable by the uncertainty in the value of $b(\text{Co})$. Shull and Wollan's value, 0.28 (29), had been revised from CoO to 0.25 (30), from Co metal and Co₃O₄ to 0.250 ± 10 (31), and from Co₃O₄ to 0.232 ± 25 (12) (all values in 10⁻¹² cm). Both 0.235 (also quoted in ref. 12) and 0.250 were tried in our refinement. An attempt was also made to include $b(\text{Co})$ as a parameter of refinement.

The results of a number of refinements can be summarized as follows. Refining for K and $x(\text{O})$ only, and putting $B(\text{overall}) = 1.00$, $b(\text{Co}) = 0.250$, gave an overall agreement which was better than for $b(\text{Co}) = 0.235$ at a significance

⁶There is a misprint in Roth's Table 1: the I_c and I_o of 622 (X-rays) cannot be 105 and 112 respectively. The values should probably be 10.5 and 11.2.

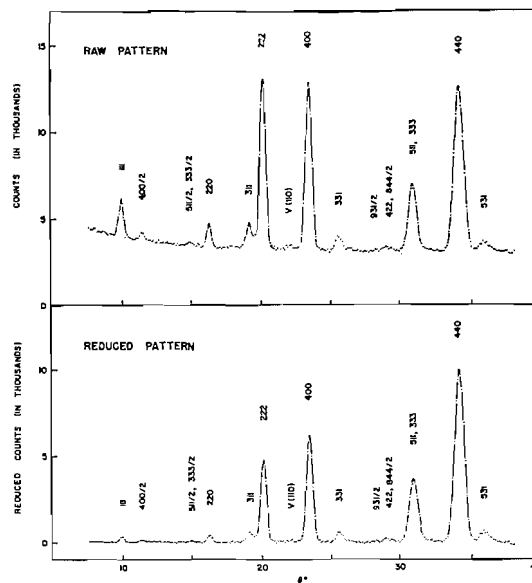


FIG. 3. Raw and reduced neutron-diffraction patterns of Co₃O₄ at room temperature (monochromator, Al(111); $\lambda = 1.60 \text{ \AA}$; average counting time per point, 20 min).

level close to 10% (33), but $x(\text{O})$ was the same in both cases, 0.2621 ± 6 . The same was true when

refining for K , $x(\text{O})$, and $B(\text{overall})$: $x(\text{O}) = 0.2624 \pm 6$, $B(\text{overall}) = 0.89 \pm 8$, $R = 1.84\%$, e.s.d.(w) = 0.062.

Attempting to refine $b(\text{Co})$ and K using best $x(\text{O})$ and $B(\text{overall})$ from the X-ray data gave $b(\text{Co}) = 0.257 \pm 11$, while with best $x(\text{O})$ and $B(\text{overall})$ from the neutron data, and starting from $b(\text{Co}) = 0.235$, gave 0.248 ± 5 .

Even though the present data are insufficient to establish a reliable value of $b(\text{Co})$, they tend to confirm Moon's value of 0.250 ± 10 . The strong parameter correlations in Co_3O_4 render $b(\text{Co})$ values derived from this compound unsatisfactory (ref. 12 and this work); Moon's results obtained with Co metal are not discussed in ref. 31 in sufficient detail to judge their reliability. Thus the value of $b(\text{Co})$ cannot be considered as settled even within the accuracy expected from such determinations.

Our best $x(\text{O})$ from neutron data, 0.2624 ± 6 , does not significantly differ from Roth's value, 0.2632 ± 4 (12), and its 2σ range overlaps with that of $x(\text{O})$ from our X-ray data.

NiCo_2O_4

The high-angle lines of the NiCo_2O_4 powder photograph were not sharp enough for a Nelson-Riley extrapolation. A 3:2 mixture by weight of NiCo_2O_4 and NiO ($a_0 = 4.1765 \pm 5 \text{ \AA}$) was therefore used to provide internal calibration. The resulting lattice parameter was within the range of values reported in the literature (Table I).

Refinement of the structure from X-ray data was less satisfactory than for Co_3O_4 . The powder pattern yielded only 11 sufficiently well-defined single reflections. Refinements based on the models $\text{Co}^{3+}[\text{Ni}^{2+}\text{Co}^{3+}]\text{O}_4^{2-}$ ($s = 0$), $\text{Co}^{2+}[\text{Ni}^{3+}\text{Co}^{3+}]\text{O}_4^{2-}$, and $\text{Ni}^{2+}[\text{Co}_2^{3+}]\text{O}_4^{2-}$ ($s = 1$), with individual isotropic temperature factors as well as with an overall temperature factor, gave results that did not significantly differ among themselves⁷. An exception was the refinement for $s = 1$ and $B(\text{overall})$. This was found rejectable, on Hamilton's \mathcal{R} criterion (33), at the 5% significance level when compared with the refinement for $s = 0$ and $B(\text{overall})$.

⁷The inversion parameter s is defined by $f(\text{M}_{\text{tetrahedral}}) = sf(\text{Ni}) + (1-s)f(\text{Co})$ and $2f(\text{M}_{\text{octahedral}}) = (1-s)f(\text{Ni}) + (1+s)f(\text{Co})$, and similarly for neutron diffraction. That is, $s = 1$ corresponds to the normal; $s = 0$, to the inverse; and $s = 1/3$, to the random (i.e. $8(a) + 16(d)$) distribution. For Co_3O_4 , read Co^{2+} for Ni and Co^{3+} for Co.

The unexpectedly close similarity of the exploratory neutron-diffraction patterns of the oxide obtained at room and liquid-nitrogen temperatures and at 120°C made it evident that the magnetic contribution to the total diffracted intensity was rather small and that unless an effort was made to ensure adequate counting statistics, attempts to interpret the magnetic structure would fail. Diffraction patterns were therefore obtained at -162 and 120°C using counting times of about 25 min per point (Fig. 4). These were judged reasonably satisfactory for Gaussian analysis, by which 10 $|F_o|$ were extracted.

The R factors calculated from the high-temperature $|F_o|$ and a reasonable set of unrefined parameter values were 12% for $s = 0$, 22% for $s = 1/3$, and 51% for $s = 1$. The best refinement of the inverse model (using $b(\text{Co}) = 0.250$) resulted in $x(\text{O}) = 0.2594 \pm 30$, $B(\text{overall}) = 0.83 \pm 42$, $R = 9.08\%$, e.s.d.(w) = 0.279. When $B(\text{overall})$ was fixed to 1.00, the same $x(\text{O})$ and R values were obtained. The values of $x(\text{O})$ and $B(\text{overall})$ agree well with the corresponding values for $s = 0$ from the X-ray data (Table II).

Attempts to refine for K and s only did not give meaningful results.

Co_3S_4

The $x(\text{S})$ for $\text{Co}[\text{Co}_2]\text{S}_4$, 0.2587 ± 6 , was very close to Lundqvist and Westgren's trial-and-error value, 0.260 (converted from -0.135 for a different choice of origin) (14). There was no significant difference between the refinement for the neutral model and for $\text{Co}^{1+}[\text{Co}^{1+}\text{Co}^{2+}]\text{S}_4^{1-}$ regardless of whether individual isotropic temperature factors or $B(\text{overall})$ were used, except that $B(\text{Co})$ of both Co atoms were positive indefinite.

To test the effect of the dispersion corrections the structure was also refined employing uncorrected neutral and singly ionic scattering factors. The results could be rejected at the 0.5% significance level when compared with those of the preceding paragraph. Thus the assumed degree of ionicity appears to affect the refinement much less than omission of the dispersion corrections.

NiCo_2S_4

Three models were used in the refinement from X-ray data: $\text{Ni}[\text{Co}_2]\text{S}_4$ ($s = 1$), $\text{Co}[\text{NiCo}]\text{S}_4$ ($s = 0$), and $(\text{NiCo}_2)\text{S}_4$ ($s = 1/3$). Since the ionicity did not appear to produce a significant difference in the refinement of Co_3S_4 , only neutral atoms were used for NiCo_2S_4 .

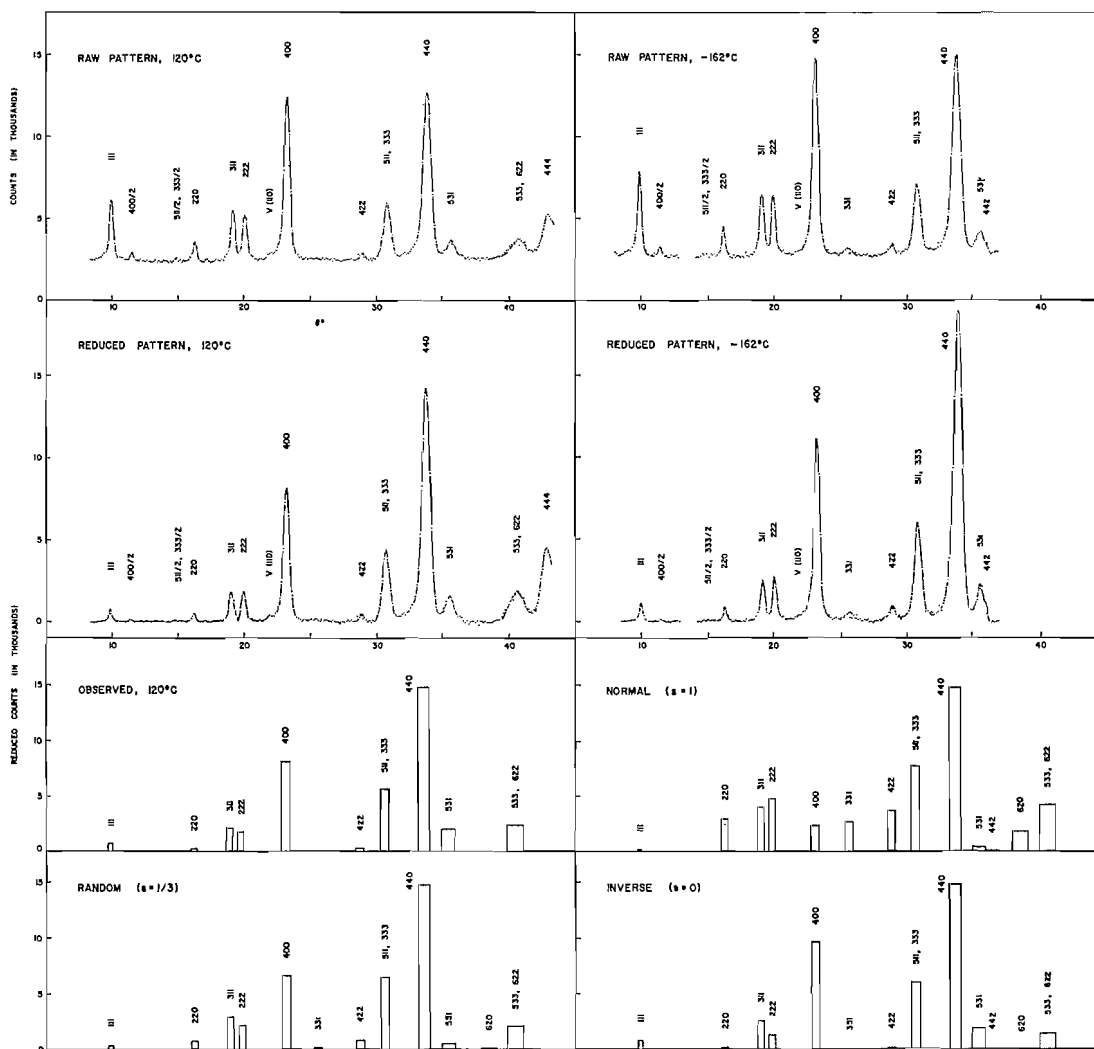


FIG. 4. Neutron-diffraction patterns of NiCo_2O_4 at 120 and -162°C (monochromator, $\text{Al}(111)$; $\lambda = 1.60 \text{ \AA}$; average counting time per point, 25 min). The two patterns have been matched in θ by correcting for thermal expansion. The histograms represent pF_o^2 (second-order contribution removed) and pF_c^2 patterns, the latter for three different cation distributions.

Assuming $s = 1$ to be the best model, the random structure ($s = 1/3$) could be rejected, on the \mathcal{R} criterion, at a significance level between 10 and 25% and the inverse structure ($s = 0$), at the 5% level. The corresponding figures for the $B(\text{overall})$ refinements were 2.5% and $<2.5\%$. There was no significant difference between the $B(\text{individual})$ and $B(\text{overall})$ refinements for $s = 1$.

In refining the structure from neutron data ($12 |F_o|$; Fig. 5) both 0.235 and 0.250 were used for $b(\text{Co})$, and beside the usually quoted $b(\text{S})$ of 0.31 (26) the value proposed by Menyuk *et al.*

(32), 0.28 ± 1 , was also tried (all values in 10^{-12} cm). R computed from a reasonable set of initial parameter values was between 12 and 15% for $s = 1$, while for $s = 1/3$ and 0 it amounted to 40% or more and could not be reduced by refining below 24%. Different combinations of $b(\text{Co})$ and $b(\text{S})$ values and $B(\text{overall}) = 0.4$ did not lead to x, K -refinements significantly different at the 25% level, although the lowest R and e.s.d.(w) values, 10.04% and 0.279 respectively, were obtained with $b(\text{Co}) = 0.25$ and $b(\text{S}) = 0.31$; the resulting $x(\text{S})$ was 0.2548 ± 44 . A three-parameter refine-

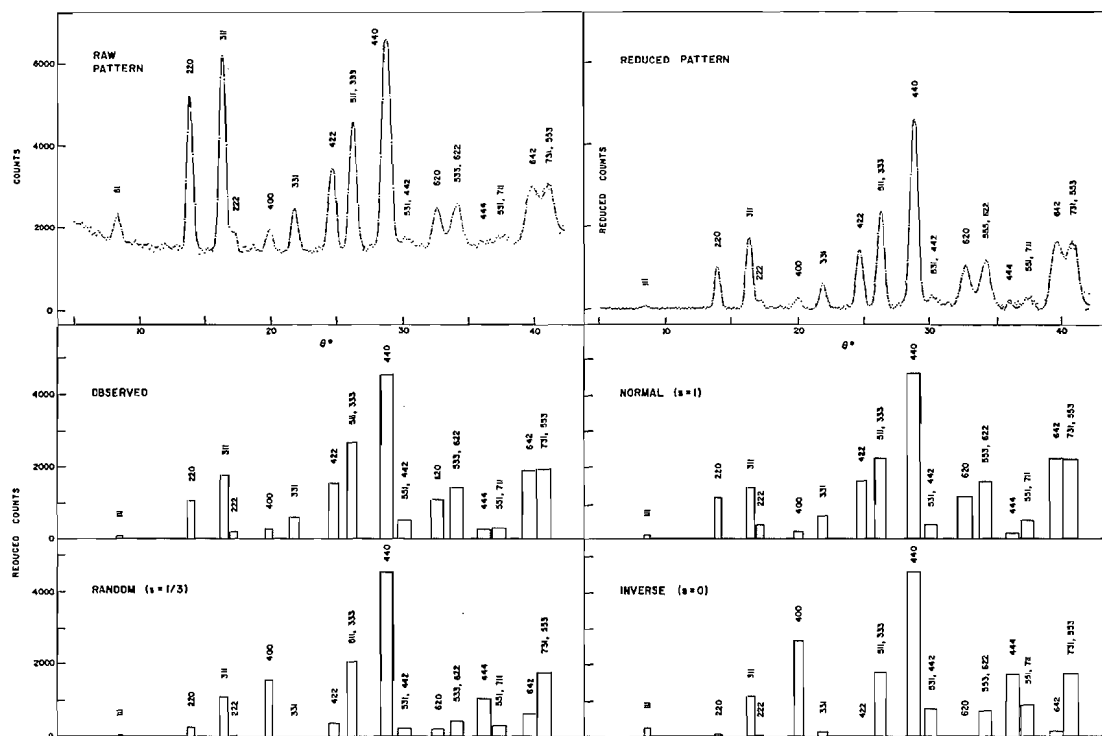


FIG. 5. Neutron-diffraction pattern of NiCo_2S_4 at room temperature (monochromator, $\text{Al}(111)$; $\lambda = 1.60 \text{ \AA}$; average counting time per point, 7 min). The second-order contribution has been removed from the pF_0^2 histogram.

ment gave $x(\text{S}) = 0.2561 \pm 47$, $B(\text{overall}) = -0.39 \pm 55$, $R = 10.69\%$, and $\text{e.s.d.}(w) = 0.288$.

Attempts to refine the normal structure for K and s were inconclusive. If anything they seemed to indicate that s might be somewhat smaller than unity. Further treatment did not appear justified because of the uncertainties in the neutron-diffraction patterns, the smaller number of usable reflections, and the relatively low scattering amplitude of S .

Magnetic Measurements

Magnetization curves of NiCo_2O_4 were measured with decreasing magnetic field at different temperatures (Fig. 6A). Hysteresis was found at low fields, i.e. the magnetizations measured with increasing fields were somewhat smaller. The temperature dependence of magnetization at 11.70 and 7.88 kOe is shown in Fig. 6B. The values of magnetization were lower than those obtained by Lotgering (4).

The magnetization was not completely saturated even in a field of 11.70 kOe, and the mag-

netization vs. T curve was of unusual shape. Since both Lotgering's and our preparations were contaminated with small amounts of foreign phases of uncertain identity⁸, it is rather difficult to estimate the "true" saturation magnetization and the Curie point. When the magnetization vs. T curve at 7.88 kOe is extrapolated to 0°K , the magnetization reaches 29.0 e.m.u./g, which corresponds to $1.25\mu_B$ per NiCo_2O_4 formula unit. Blasse (34) obtained, from Lotgering's data, the value of $1.5\mu_B$ and also estimated, by extrapolating a linear portion of the magnetization vs. T curve to zero magnetization, the Curie point as 350°K . This value seems, however, incorrect because the magnetizations at 460°K are not yet proportional to magnetic fields (Fig.

⁸Lotgering suggests that the foreign phase in his specimen may have been NiO . If so, Co_3O_4 would also have been present, and possibly CoO as well; the lower oxide may in fact have been a solid solution $(\text{Ni},\text{Co})\text{O}$. Quite apart from the presence of foreign phases the magnetic properties of NiCo_2O_4 itself may depend on its exact stoichiometry and on the details of preparation. Lotgering's report that the $1/\chi$ vs. T curve was reversible up to 800°C further complicates the situation.

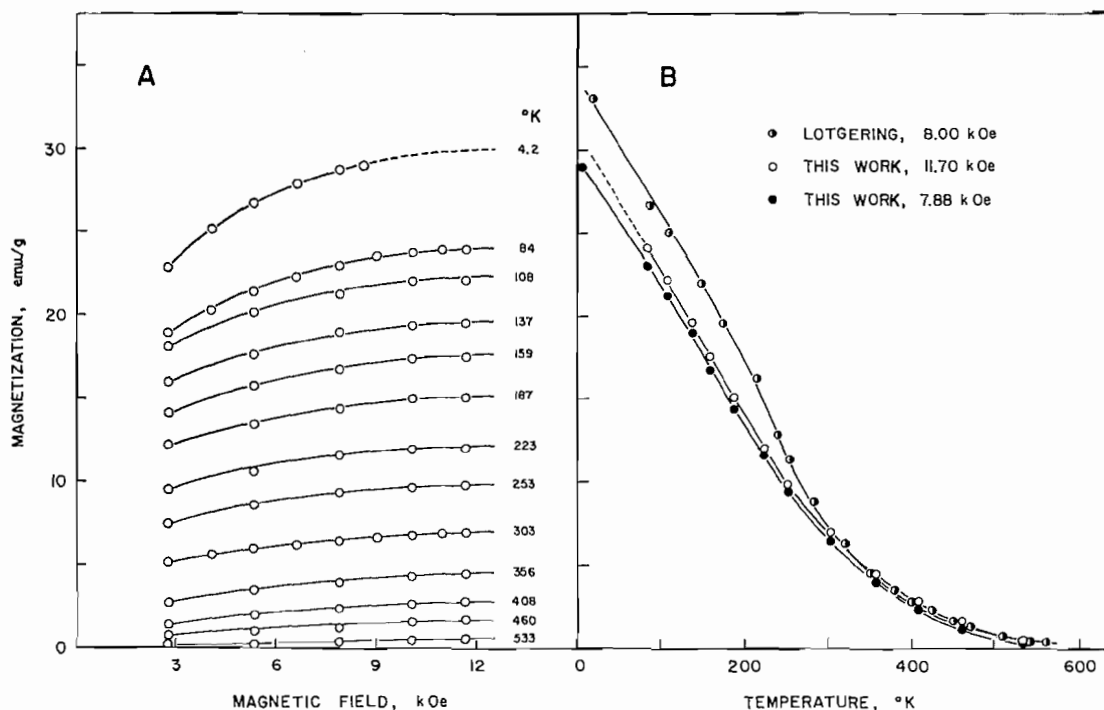


FIG. 6. (A) Field dependence of the magnetization of NiCo_2O_4 at different temperatures (measured with decreasing magnetic field). (B) Temperature dependence of the magnetization of NiCo_2O_4 at 7.88 and 11.70 kOe. Lotgering's data are reproduced from Fig. 4 of ref. 4.

6A). The true Curie point would be expected to lie in the vicinity of 500 °K.

There is little doubt that NiCo_2O_4 is not simply ferromagnetic but ferrimagnetic. The anomalous magnetization vs. T curve suggests the occurrence of Néel's R -type of ferrimagnetism (35), in which one of the two sublattice magnetizations is not completely aligned⁹.

Magnetic Contribution to the Neutron-Diffraction Pattern of NiCo_2O_4

Compared with the corresponding NiCo_2O_4 pattern at 120 °C the reduced (pF_o^2) pattern at -162 °C showed the expected overall increase in intensity, and the 331 and 422 maxima were sharper, but no separate magnetic peaks were

⁹Strictly speaking Néel's theory of R -type ferrimagnetism is incomplete. Either the triangular spin configuration proposed by Yafet and Kittel (36) or the ferrimagnetic spiral configuration similar to that of MnCr_2O_4 (37) may be realized in the present case. The results of neutron-diffraction experiments, however, are insufficient to establish these nonlinear spin arrangements. Néel's R -type arrangement may be regarded as the first approximation of such arrangements.

observed (Fig. 4). The magnetic unit cell at -162 °C thus appears to coincide with the chemical unit cell.

To determine the magnetic contribution to the total diffraction intensity at -162 °C, the integrated reduced intensities at the two temperatures of 5 reflections at low Bragg angles were evaluated by Gaussian analysis and the second-order contributions were removed. The values of the ratio $r = F_o^2(111 \text{ °K})/F_o^2(393 \text{ °K})$ are shown in Table IV.

Since the two patterns were not obtained under the same conditions, the two sets of pF_o^2 were normalized to 440, in which the magnetic contribution to the observed intensity should be negligibly small: $r_0 = (r/t)(t_{440}/r_{440}) = F_o^{*2}(\text{total})/F_o^{*2}(\text{nuclear})$, where F_o^* are temperature-independent structure factors and $t = \exp[-(B_{111} - B_{393}) \sin^2 \theta/\lambda^2]$. The temperature factors were estimated by assuming the oxide to behave like an isotropic Debye solid with a characteristic temperature Θ of 400 °K. This value would correspond to a B_{293} of approximately 0.6 \AA^2 ; t

TABLE III
Observed and calculated structure factors (X-ray and neutron data)

<i>hkl</i>	$\text{Co}^{2+}[\text{Co}_2^{3+}]\text{O}_4^{2-}$		$\text{Co}^{3+}[\text{Ni}^{2+}\text{Co}^{3+}]\text{O}_4^{2-}$		$\text{Co}[\text{Co}_2]\text{S}_4$		$\text{Ni}[\text{Co}_2]\text{S}_4$	
	$10 F_o $	$10 F_c$	$10 F_o $	$10 F_c$	$10 F_o $	$10 F_c$	$10 F_o $	$10 F_c$
	X-Rays (individual temperature factors)							
111	793	799	754	761	918	939	856	879
220	1599	-1631	1420	-1516	1746	-1740	1879	-1831
311	2426	-2415	2388	-2470	2600	-2640	2669	-2703
222	1186	1136	1371	1252	433	-566	505	-524
400	2739	2793	3023	2956	4983	4935	4865	4839
331	—	-84	—	-318	—	37	—	81
422	1105	1133	1026	1089	1296	1340	1420	1403
440	4044	3992	4171	3972	6563	6523	6508	6544
531	397	-357	403	-440	597	-566	479	-547
442	—	103	—	25	—	132	—	135
620	818	836	*	813	1074	1077	1101	1114
533	1537	-1496	†	-1460	1781	-1874	1902	-1916
622	1068	1103	†	1145	—	-262	—	-164
444	1489	1475	1472	1581	3402	3455	3510	3390
551‡	559	550	*	468	1012	1022	990	1014
642	782	-781	616	-659	1060	-1110	1129	-1132
800	2427	2489	2224	2419	5076	4998	4999	4969
733	—	—	—	—	*	-550	*	-521
644	—	—	—	—	—	106	—	106
662	—	—	—	—	—	-318	—	-183
840	—	—	—	—	2758	2776	2671	2728
911§	—	—	—	—	—	—	883	855
	Neutrons (<i>K</i> , <i>x</i> , <i>B</i> (overall))							
111	29	27	47	53	—	—	27	-33
220	22	-24	23	-21	—	—	86	-84
311	24	-26	51	-56	—	—	82	-77
222	133	-133	86	-77	—	—	47	-59
400	185	186	239	249	—	—	64	57
331	24	26	—	—	—	—	50	49
422	12	15	18	15	—	—	81	84
440	205	204	273	266	—	—	220	227
531	23	-23	55	-48	—	—	37	34
620	—	—	—	—	—	—	108	84
533	—	—	75	-53	—	—	—	—
622	—	—	50	-61	—	—	—	—
444	—	—	—	—	—	—	68	56
642	—	—	—	—	—	—	72	-90

*Observed but not counted.

†533 and 622 could not be resolved.

‡Actually 551 + 711, but $I_o(711)$ negligible.

§Actually 911 + 753, but $I_o(753)$ negligible.

is relatively insensitive to variations in Θ . The experimental value of F_o^* (magnetic) can then be obtained from $q^{-2}(r_0 - 1) F_o^{*2}$ (nuclear), where $q^2 = 2/3$. Instead of F_o^{*2} (nuclear) the corresponding calculated values were employed (Table IV).

The magnetic scattering amplitudes used in the calculation of the theoretical values of F^* (magnetic) were $p_A = 0.269 f_A M_A$ for the cations in the 8(*a*) sites and $p_B = 0.269 f_B M_B$ for the cations in the 16(*d*) sites. The magnetic form factors, f_A and f_B , were tentatively chosen to be the mean values of $f(\text{Ni}^{2+})$ and $f(\text{Co}^{2+})$ given by Scatturin

et al. (38), so that $f_A = f_B = f$. Little difference resulted when Watson and Freeman's theoretical ($\langle j_0 \rangle$ only) form factors (39) were employed.

The saturation magnetization at 111 °K was found from the magnetic-balance measurements to be approximately $0.9 \mu_B$ per formula unit (Fig. 6). The effective magnetic moments must thus satisfy the relation $M_A + 2M_B = 0.9 \mu_B$. In order to obtain reasonable results they must be assumed to have opposite signs ($M_A > 0$, $M_B < 0$), i.e. NiCo_2O_4 is ferrimagnetic.

The theoretical values of F^{*2} (magnetic) for three combinations of M_A and M_B values are

TABLE IV
Comparison of theoretical and experimental magnetic structure factors for NiCo₂O₄ at 111 °K*

hkl	f	r	r ₀	F _c * ² (nuclear)/16	F* ² (magnetic)/16			
					Exptl.	Theoretical		
						M _A = 1.5 M _B = -0.3	1.7 -0.4	1.9 -0.5
111	0.91	1.51 ± 0.02	1.22	1.86	0.61 ± 0.06	0.44	0.61	0.81
220	0.80	3.66 ± 1.30	2.90	0.29	0.83 ± 0.57	0.42	0.53	0.67
311	0.74	1.40 ± 0.01	1.10	2.10	0.30 ± 0.03	0.09	0.10	0.11
222	0.73	1.36 ± 0.01	1.06	3.92	0.35 ± 0.06	0.06	0.10	0.15
400	0.68	1.34 ± 0.01	1.03	42.6	1.91 ± 0.64	0.59	0.83	1.12
440	0.52	1.36 ± 0.01	1.00	53.7	0.0 ± 0.8	0.06	0.06	0.06

*The uncertainty limits of *r* are based on the assumption that the estimate of the second-order contamination of the diffracted beam was in error by 12%.

shown in Table IV. The uncertainty limits of the corresponding experimental values were estimated from an assumed error of 12% in the estimate of the second-order contamination, but there are other sources of uncertainty. The magnetic form factor is approximate; $\chi(O)$ may vary with temperature; the exact degree of inversion is not known; and as the discrepancy in Lotgering's and our magnetization curves shows, the value of the saturation magnetization at 111 °K must be viewed with caution. The poor crystallinity of the oxide and the presence of small amounts of impurity phases in both investigations must have affected all the measurements to a varying degree.

Taking all these factors into account, the agreement of the $F^{*2}(\text{magnetic})$ at 111 °K (Table IV) is not unreasonable. The best values of M_A and M_B would appear to be 1.9 ± 0.2 and -0.5 ± 0.1 bohr magnetons. They would be larger at lower temperatures.

Blasse (34) suggested that the ionic structure of NiCo₂O₄ might be Co²⁺[Ni³⁺Co³⁺]O₄, with Co²⁺ in a high-spin state ($M_A = 3 \mu_B$) and Ni³⁺ and Co³⁺ both in low-spin states ($M_B = 0.5 \mu_B$). Assuming the spin moments at 0 °K to be antiparallel and completely collinear, the net magnetization would be $2 \mu_B$. The values found by experiment, however, were only $1.5 \mu_B$ (4, 34) and $1.25 \mu_B$ (this work) respectively. Even if the estimates of the saturation magnetization at 0 °K are in error by as much as 20%, the alignment of the spin moments cannot be complete.

Another possible structure is Co³⁺[Ni²⁺Co³⁺]O₄, with the Co³⁺ ions in 8(*a*) and 16(*d*) in high ($4 \mu_B$) and low ($0 \mu_B$) spin states respectively. The Ni²⁺ ion has a moment of $2 \mu_B$ regard-

less of the strength of the crystal field. The net magnetization would be the same as that of the arrangement proposed by Blasse.

The results of the neutron-diffraction study are not inconsistent with either model. The numerous unfavorable factors inherent in an investigation of NiCo₂O₄ preclude other models of the magnetic structure to be meaningfully tested. But the applicability of such models (e.g. Yafet-Kittel triangular arrangement or screw-type ferrimagnetism) might be investigated on an improved set of experimental data. It should be possible to increase the crystallinity of the oxide by high-pressure annealing in oxygen above 300 °C. The magnetic contribution could be increased and evaluated with more certainty from neutron-diffraction experiments at 4.2 and 500 °K on reducing the second-order component of the beam to a negligible value, and it could be separated, at liquid-helium temperatures, from the nuclear contribution by applying an external magnetic field.

Interatomic Distances

The apparent M—O and M—S distances in the cobaltites are compared with similar distances in simple oxides and sulfides of Co and Ni in Table V. The effective size of the 3*d* atom (or ion) depends not only on its oxygen or sulfur coordination but, as would be expected, also on its spin configuration (cf. ref. 48). The distances cannot be meaningfully compared unless the spin states are known with certainty and the respective spin sublattices are clearly defined. Unfortunately the compounds for which this information is available and which are otherwise

TABLE V
Interatomic distances, in Å, in the cobaltites and other compounds*

Distance	Tetrahedral coordination	Octahedral coordination
Co ²⁺ —O	Co ²⁺ [Co ³⁺]O ₄ (h.s.): 1.946 ± 34 (this work)	CoO (B1, h.s.): 2.1290 ± 5 (40) 2.1301 ± 5 (41)
Co ³⁺ —O		Co ²⁺ [Co ³⁺]O ₄ (l.s.): 1.915 ± 18 (this work)
Ni ²⁺ —O		NiO (B1, h.s.): 2.0973 ± 5 (275 °C) (42) 2.0894(±6) (300 °K) (43)
Co—S	Co[Co ₂]S ₄ : 2.184 ± 23 (this work)	Co[Co ₂]S ₄ (l.s.? Cf. refs. 15 and 49): 2.268 ± 13 (this work)
	Co ₉ S ₈ (1 S+3 S): 2.13 ± 5; 2.21 ± 2 (44) 2.119; 2.212 (45)	Ni[Co ₂]S ₄ : 2.265 ± 7 (this work)
		Co ₉ S ₈ : 2.39 ± 3 (44) 2.392 (45)
Ni—S	Ni[Co ₂]S ₄ : 2.179 ± 12 (this work)	CoS ₂ (C2, l.s. ? Cf. ref. 51): 2.317(±7) (46)
	Ni ₃ S ₂ : 2.28 (kX ?) (47)	NiS ₂ (C2): 2.396(±15) (46)

*h.s., high spin; l.s., low spin. Values quoted as "this work" have not been corrected for thermal motion. They are based on weighted averages of $x(X)$ from X-ray refinements for B (individual) and B (overall) and their uncertainty limits refer to $3\sigma(x)$ and $2\sigma(a_0)$.

suitable for comparisons are few, but some observations can still be made (Table V):

(1) The Co²⁺—O distance (Co²⁺ in a high-spin state, $d_e^5 d_\gamma^2$) for octahedral coordination (in CoO) is about 0.185 ± 55 Å, i.e. ca. 9%, greater than for tetrahedral coordination (in Co₃O₄).

(2) The difference in the lattice parameters of Co₃S₄ and Ni[Co₂]S₄ is only 0.019 ± 4 Å, and the $x(S)$ values are identical. The M—S distances in the two spinels thus cannot be significantly different, and the spin states of the Co(VI) atom will be the same.

(3) Co₃O₄ at room temperature is known to have the ionic arrangement (h.s., high spin; l.s., low spin) Co_{h.s.}²⁺[Co_{l.s.}³⁺]₂O₄ (12). If the distribution Co_{h.s.}²⁺[Ni_{l.s.}³⁺Co_{l.s.}³⁺]O₄ proposed by Blasse is correct, the M(IV)—O distances in Co₃O₄ and NiCo₂O₄ should be closely similar, but the M(VI)—O distance in NiCo₂O₄ should be greater than the corresponding distance in Co₃O₄, the low-spin Ni³⁺ ion being larger than low-spin Co³⁺ (48). If on the other hand the distribution is Co_{h.s.}³⁺[Ni_{h.s.}²⁺Co_{l.s.}³⁺]O₄, the M(IV)—O distance in NiCo₂O₄ should be shorter than the corresponding distance in Co₃O₄, and the M(VI)—O distance in NiCo₂O₄ should be longer than in Co₃O₄, Ni_{h.s.}²⁺ being larger than Co_{l.s.}³⁺. The observed distances in NiCo₂O₄ were 1.874 ± 127 Å for M(IV)—O and 1.963 ± 81 Å for M(VI)—O, but because of the large uncertainty limits neither value can be invoked in support of a particular distribution.

(4) The Co(IV)—S distance in Co₃S₄, 2.184 Å, is the same as the average of the four Co(IV)

—S distances in Co₉S₈, while the Co(VI)—S distance in the spinel, 2.268 Å, is more than 5% shorter than the corresponding distance in Co₉S₈, but only about 2% shorter than the Co(VI)—S distance in the pyrite-type CoS₂.

Conclusions

The combined results of the X-ray and neutron-diffraction investigation of the two ternary spinels show that NiCo₂O₄ is inverse, while NiCo₂S₄ is normal. It was surprising to see that refinements of NiCo₂S₄ from the rather limited volume of data provided by X-ray powder diffractometry were capable of distinguishing between models based on normal and inverse distributions.

The best values of the positional parameters of the oxygen or sulfur atoms obtained from the present X-ray data were: Co₃O₄, 0.2640 ± 8; NiCo₂O₄, 0.2583 ± 34; Co₃S₄, 0.2591 ± 5; NiCo₂S₄, 0.2591 ± 3 (weighted averages from B (individual) and B (overall) refinements).

The volume of diffraction data was too small for a reliable determination of the degree of inversion in NiCo₂O₄ and NiCo₂S₄. When NiCo₂O₄ and NiCo₂S₄ were refined for assumed values of the inversion parameter s , the $x(O)$ and $B(X)$ tended to vary with s but they moved in the opposite directions. The importance of this behavior is obscured by the large e.s.d.'s of the final parameter values of NiCo₂O₄, but in future refinements from more accurate intensity data the interdependence of the positional and thermal parameters and the degree of inversion will have to be recognized. A related problem has been

considered by Anishchenko *et al.* (50), who investigated the effect of the shape of the f -curves (as dependent on the effective crystal radii) on the determination of $x(O)$ and the degree of inversion in $MgFe_2O_4$. They have pointed out that in order to determine these two quantities the experimental intensities must be accurate to 0.1%, and the location of all the ions must be known (i.e. occupancy of sites other than the classical spinel equipoints 8(a) and 16(d) must be investigated).

The segregation of the Ni atoms in the tetrahedral sites of the $NiCo_2S_4$ structure contrasts with the indifference of the Ni and Co atoms in the cubic π phase Co_8NiS_8 to a particular type of coordination. It may be just as much the result of a strong preference of Ni in the sulfospinel for tetrahedral coordination as a manifestation of a tendency of Co to occupy octahedral sites.

As regards the choice between the alternative cation distributions in $NiCo_2O_4$ that have been considered in this work, the present evidence is inconclusive. The results of magnetization measurements and the magnetic contribution to Bragg scattering at 111 °K are compatible with both models. Additional work is needed to clarify this point.

Acknowledgments

We wish to express our gratitude to the staff of the Neutron Physics Branch, Atomic Energy of Canada Limited, for placing at our disposal their neutron diffraction facilities; to Dr. F. Brisse, Mrs. E. J. Payne, and Mr. H. Nieman for assistance with the experimental work; to Mr. H. Suzuki, Institute for Solid State Physics, Tokyo, for the measurements at liquid-helium temperatures; and to Dr. N. F. H. Bright and Mr. R. H. Lake, Mineral Sciences Division, Mines Branch, Department of Energy, Mines and Resources, Ottawa, Canada, for obtaining the d.t.a. curves of the oxides.

This investigation was supported by grants in aid of research from the National Research Council of Canada and the Geological Survey of Canada to the first-named author.

1. O. KNOP and M. A. IBRAHIM. *Can. J. Chem.* **39**, 297 (1961).
2. S. HOLGERSSON and A. KARLSSON. *Z. Anorg. Allgem. Chem.* **183**, 384 (1929).
3. J. ROBIN and C. BÉNARD. *Compt. Rend.* **232**, 1830 (1951); **234**, 734, 956 (1952).
4. F. K. LOTGERING. *Philips Res. Rept.* **11**, 190, 337 (1956).
5. S. B. HENDRICKS and W. H. ALBRECHT. *Ber.* **61B**, 2153 (1928).
6. G. NATTA and M. STRADA. *Gazz. Chim. Ital.* **58**, 419 (1928).
7. S. HOLGERSSON. *Lunds Univ. Arsskr. Avd. 2*, **23**, 9 (1929); *Kgl. Fysiograf. Sällskap. Lund Handl.* **38**, 1 (1929).
8. O. KRAUSE and W. THIEL. *Ber. Deut. Keram. Ges.* **15**, 101 (1934).
9. H. E. SWANSON, M. I. COOK, T. ISAACS, and E. H. EVANS. *Natl. Bur. Std. U.S. Circ. No.* 539, **9**, 29 (1960).
10. P. COSSEE. Ph.D. Thesis, Leiden, 1956 (quoted from ref. 17).
11. R. J. MAKKONEN. *Suomen Kemistilehti, B*, **35**, 230 (1962).
12. W. L. ROTH. *Phys. Chem. Solids*, **25**, 1 (1964).
13. W. F. DE JONG and H. W. V. WILLEMS. *Z. Anorg. Allgem. Chem.* **161**, 311 (1927).
14. D. LUNDQVIST and A. WESTGREN. *Z. Anorg. Allgem. Chem.* **239**, 85 (1938).
15. R. J. BOUCHARD, P. A. RUSSO, and A. WOLD. *Inorg. Chem.* **4**, 685 (1965).
16. P. COSSEE. Private communication.
17. G. BLASSE. *Philips Res. Rept. Suppl.* **3**, (1964).
18. O. KNOP, F. BRISSE, L. CASTELLIZ, and SUTARNO. *Can. J. Chem.* **43**, 2812 (1965).
19. F. BRISSE and O. KNOP. *Can. J. Chem.* **45**, 609 (1967).
20. S. GOCAN. *Acad. Rep. Populare Romine, Filiala Iasi, Studii Cercetari Stiint. Fiz. Stiinte Tehn.* **14**(2), 393 (1963).
21. SUTARNO, O. KNOP, and K. I. G. REID. *Can. J. Chem.* **45**, 1391 (1967).
22. F. R. AHMED, E. J. GABE, G. A. MAIR, and M. E. PIPPY. A unified set of crystallographic programs for the IBM 1620 computer. September 1963. Unpublished.
23. *International tables for X-ray crystallography. Vol. III.* Kynoch Press, Birmingham, 1962.
24. M. TOKONAMI. *Acta Cryst.* **19**, 486 (1965).
25. D. T. CROMER. *Acta Cryst.* **18**, 17 (1965).
26. G. E. BACON. *Neutron diffraction*. 2nd ed. Oxford University Press, Oxford, 1962.
27. T. HIRONE, S. MAEDA, and N. TSUYA. *Rev. Sci. Instr.* **25**, 516 (1954).
28. F. BRISSE and O. KNOP. *Can. J. Chem.* **46**, 859 (1968).
29. C. G. SHULL and E. O. WOLLAN. *Phys. Rev.* **81**, 527 (1951).
30. W. L. ROTH. *Phys. Rev.* **110**, 1333 (1958).
31. R. M. MOON. *Phys. Rev.* **136**, A195 (1964).
32. N. MENYUK, K. DWIGHT, and A. WOLD. *J. Appl. Phys.* **36**, 1088 (1965).
33. W. C. HAMILTON. *Acta Cryst.* **18**, 502 (1965).
34. G. BLASSE. *Philips Res. Rept.* **18**, 383 (1963).
35. L. NÉEL. *Ann. Phys. [12]* **3**, 137 (1948).
36. Y. YAFET and C. KITTEL. *Phys. Rev.* **87**, 290 (1952).
37. L. M. CORLISS and J. M. HASTINGS. *Phys. Rev.* **126**, 556 (1962).
38. V. SCATTURIN, L. M. CORLISS, N. ELLIOTT, and J. M. HASTINGS. *Acta Cryst.* **14**, 19 (1961).
39. R. E. WATSON and A. J. FREEMAN. *Acta Cryst.* **14**, 27 (1961).
40. N. C. TOMBS and H. P. ROOKSBY. *Nature*, **165**, 442 (1950).
41. R. E. CARTER and F. D. RICHARDSON. *J. Metals*, **7**, 336 (1955).
42. H. P. ROOKSBY. *Acta Cryst.* **1**, 226 (1948).
43. V. S. KOGAN and T. G. OMAROV. *Zh. Eksperim. Teor. Fiz.* **47**, 789 (1964).

44. S. GELLER. *Acta Cryst.* **15**, 1195 (1962).
45. SUTARNO. Ph.D. Thesis, Nova Scotia Technical College, Halifax, N.S. 1965.
46. N. ELLIOTT. *J. Chem. Phys.* **33**, 903 (1960).
47. A. WESTGREN. *Z. Anorg. Allgem. Chem.* **239**, 82 (1938).
48. G. BLASSE. *J. Inorg. Nucl. Chem.* **27**, 748 (1965).
49. G. BLASSE. *Phys. Letters*, **19**, 110 (1965).
50. R. I. ANISHCHENKO, E. G. BOGACHEVA, and A. N. MEN'. *Dokl. Akad. Nauk SSSR*, **171**, 573 (1966).
51. A. F. ANDRESEN, S. FURUETH, and A. KJEKSHUS. *Acta Chem. Scand.* **21**, 833 (1967).